International Scholarly Research Network
ISRN Applied Mathematics
Volume 2011, Article ID 532682, 19 pages
doi:10.5402/2011/532682

Research Article

Acoustic Wave Propagation in a Trifurcated Lined Waveguide

M. Ayub, M. H. Tiwana, A. B. Mann, and H. Zaman

Department of Mathematics, Quaid-i-Azam University, Islamabad 44000, Pakistan

Correspondence should be addressed to M. Ayub, mayub59@yahoo.com

Received 11 March 2011; Accepted 30 March 2011

Academic Editors: C. Chen, P. J. García Nieto, and C. Lu

The diffraction of sound from a semi-infinite soft duct is investigated. The soft duct is symmetrically located inside an acoustically lined but infinite duct. A closed-form solution is obtained using integral transform and Jones' method based on Wiener-Hopf technique. The graphical results are presented, which show how effectively the unwanted noise can be reduced by proper selection of different parameters. The kernel functions are factorized with different approaches. The results may be used to design acoustic barriers and noise reduction devices.

1. Introduction

The analysis of the effects of unwanted noise has been an active area of research because of its technological importance. This study is important in connection with exhaust system, steam valves, internal combustion engines of aircraft and vehicles, turbofan engines, and ducts and pipes. The analysis of wave scattering by such structures is an important area of noise reduction and relevant for many applications. Continued interest in the problem of noise reduction has attracted the attention of many scientists, physicists, and numerical simulists.

Many interesting mathematical models for the reduction of noise are discussed by several authors. In view of historical perspectives the story goes that Rawlins [1] was the first to show that the duct with a thin acoustically absorbent lining is an effective method which can be used to reduce the unwanted noise within a waveguide. As a sound attenuator, the acoustic performance of a duct can be increased significantly by lining its walls with an acoustically absorbent material [2]. Koch [3] discussed the problem of noise reduction from the engineering point of view, namely, in rectangular chambers, circular and annular geometries in the absence of mean flow situation. In another paper [4], Koch discussed

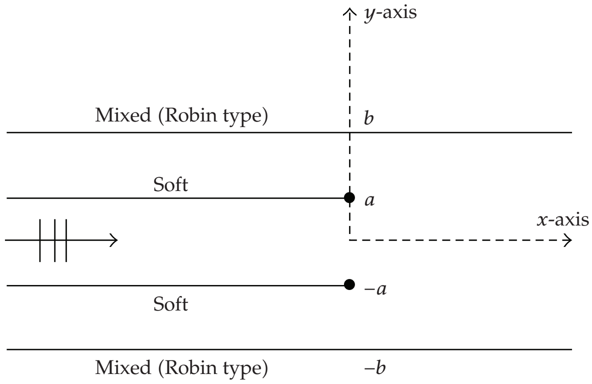

Figure 1: Schematic diagram of the trifurcated waveguide.

the analytical solution of the problem of sound radiation from the open end of a semi-infinite two-dimensional duct whose inner side walls are lined with a locally reacting sound absorbing material of finite length. The problem was solved analytically with the help of Wiener-Hopf technique. The obtained analytical results were also discussed numerically for several parameters of interest.

Jones [5] discussed the problem of scattering of plane waves from three parallel soft semi-infinite and equidistant plates and calculated the far field and the field within the waveguide. Later on, Asghar et al. [6] extended Jones analysis [5] for the case of line source and point source scattering in still air and as the medium is convective. Afterwards Hassan and Rawlins [7] analyzed an acoustic diffraction problem considering a semi-infinite hard-soft duct and obtained exact, closed-form solution valid for all plate spacings. Asghar and Hayat [8] obtained an exact solution for the problem of scattering of sound within absorbing parallel plates using Wiener-Hopf technique. In [9] the analytical solution of the sound field of a semi-infinite acoustically soft cylindrical duct, accounting for diffraction at the outlet, has been obtained applying Wiener-Hopf technique. In a similar context, Büyükaksoy and Polat [10] studied diffraction phenomenon in a bifurcated waveguide by considering a dominant mode wave incident on a soft-hard half-plane centered inside an infinite parallel plate waveguide with hard boundaries.

Related work regarding the diffraction of dominant acoustic wave modes from the trifurcated waveguide having the same geometric design but with different combinations of the boundary conditions (soft, hard, mixed (Robin type)) in the case of still air and for convective flow may be found in [11–14]. Keeping in view of the importance of the above-mentioned configuration, in this paper we have attempted to solve the problem of diffraction of a dominant acoustic mode propagation out of the mouth of a semi-infinite soft duct which is symmetrically located within an infinite lined duct on which general third-type mixed boundary conditions of the Robin type are satisfied. The boundary value problem is solved analytically with the help of standard Wiener-Hopf procedure based on Jones' method, more mechanical and straightforward, rather than by using the cumbersome integral equation apparatus. This method has applications in almost all modern branches of science, engineering, and technology. For more details one is referred to [15, 16]. The geometry of the trifurcated waveguide problem under consideration is shown in Figure 1, and the paper is organized as follows.

The problem statement is presented in Section 2. The Wiener-Hopf (WH) equation is formed in Section 3. The problem is further solved in Section 4. The solution procedure involves the complex contour integrals. These integrals are evaluated in Section 5 by an application of Cauchy residue theorem [17]. The explicit factorization of the Wiener-Hopf kernel function is accomplished in the appendix. Numerical and graphical results are also presented.

2. Problem Statement

The physical situation considered is that of the diffraction of first mode of the inside waveguide (which is the only propagative mode) as incident mode that propagates out of the end of a semi-infinite soft duct. The wave mode is propagating in the positive x-direction parallel to x-axis. The semi-infinite soft duct is placed inside the absorbingly lined duct. If $\phi(x, y, t)$ is a scalar potential, then the velocity $\mathbf{u}$ and acoustic pressure p can be written as

$$\begin{aligned} \mathbf{u} &= \operatorname{grad} \phi, \\ p &= -\rho_o \frac{\partial \phi}{\partial t}, \end{aligned} \tag{2.1}$$

respectively, where grad is the gradient operator, ρ_o is the density, and t is the time. Writing

$$\phi(x, y, t) = e^{-i\omega t} \Phi(x, y) \tag{2.2}$$

and omitting $e^{-i\omega t}$ throughout, we have to solve the following Helmholtz equation:

$$\frac{\partial^2 \Phi}{\partial x^2} + \frac{\partial^2 \Phi}{\partial y^2} + k^2 \Phi = 0, \tag{2.3}$$

where $k = \omega / c$ (ω is the angular frequency and c is the speed of sound) is the wave number.

The boundary conditions and continuity conditions associated with the problem are of the form

$$\Phi + \left(\frac{i\zeta}{k}\right) \frac{\partial \Phi}{\partial y} = 0, \quad y = b, \ -\infty < x < \infty, \tag{2.4}$$

$$\Phi = 0, \quad y = a, \ -\infty < x < 0, \tag{2.5}$$

$$\Phi = 0, \quad y = -a, \ -\infty < x < 0, \tag{2.6}$$

$$\Phi - \left(\frac{i\zeta}{k}\right) \frac{\partial \Phi}{\partial y} = 0, \quad y = -b, \ -\infty < x < \infty, \tag{2.7}$$

$$\frac{\partial}{\partial y} \Phi(x, -a^+) = \frac{\partial}{\partial y} \Phi(x, -a^-), \quad x > 0, \tag{2.8}$$

$$\frac{\partial}{\partial y} \Phi(x, a^+) = \frac{\partial}{\partial y} \Phi(x, a^-), \quad x > 0, \tag{2.9}$$

where it is assumed that $b > a$. In (2.4) and (2.7), ζ represents the specific impedance of the infinite duct lining and it is necessary that for an absorbent surface $\operatorname{Re}\zeta > 0$.

Besides the conditions prescribed in (2.4)–(2.9), we require those conditions at infinity which are relevant to the nature of the lowest propagating modes in various duct regions. The radiation conditions at infinity suggest the following [14].

For the region $(-a \le y \le a, x < 0)$, one may write

$$\Phi(x,y) = e^{i\chi_1 x}\sin\left[\frac{\pi(y-a)}{2a}\right] + \sum_{n=1}^{\infty} R_n e^{-i\chi_n x}\sin\left[\frac{n\pi(y-a)}{2a}\right], \tag{2.10}$$

where $\chi_n = (k^2 - \alpha_n^2)^{1/2}$, $(n = 1,2,3,\ldots,)$ and α_n satisfy

$$\sin 2(\alpha_n a) = 0, \tag{2.11}$$

$\alpha_n = n\pi/2a$ with $0 < \operatorname{Im}\chi_1 < \operatorname{Im}\chi_2 < \operatorname{Im}\chi_3 \ldots$. The lowest-order plane wave mode can propagate only when $\pi/2 < ka < \pi$.

The value of $\Phi(x,y)$ for $(-b \le y \le b,\ x > 0)$ is

$$\Phi(x,y) = \sum_{n=1}^{\infty} T_n e^{i\sigma_n x}\left[-\sin\beta_n(y-b) + \frac{i\zeta}{k}\beta_n\cos\beta_n(y-b)\right], \tag{2.12}$$

where $\sigma_n = (k^2 - \beta_n^2)^{1/2}$ $(n = 1,2,3,\ldots)$ and β_n satisfy the equation

$$\sin 2(b\beta_n) + 2i\beta_n\frac{\zeta}{k}\cos 2(b\beta_n) + \beta_n^2\frac{\zeta^2}{k^2}\sin 2(b\beta_n) = 0, \tag{2.13}$$

with $0 < \operatorname{Im}\sigma_1 < \operatorname{Im}\sigma_2 < \operatorname{Im}\sigma_3 \ldots$.

For $(a \le y \le b,\ x < 0)$ one has

$$\Phi(x,y) = \sum_{n=1}^{\infty} \widetilde{T}_n e^{-i\widetilde{\alpha}_n x}\left[-\sin\delta_n(y-b) + \frac{i\zeta}{k}\delta_n\cos\delta_n(y-b)\right], \tag{2.14}$$

where $\widetilde{\alpha}_n = (k^2 - \delta_n^2)^{1/2}$ $(n = 1,2,3,\ldots)$ and δ_n represent the roots of the equation

$$\sin\delta_n(b-a) + \frac{i\varsigma}{k}\delta_n\cos\delta_n(b-a) = 0, \tag{2.15}$$

with $0 < \operatorname{Im}\widetilde{\alpha}_1 < \operatorname{Im}\widetilde{\alpha}_2 < \operatorname{Im}\widetilde{\alpha}_3 \ldots$.

When $(-b \le y \le -a,\ x < 0)$, we have

$$\Phi(x,y) = \sum_{n=1}^{\infty} \widehat{T}_n e^{-i\widehat{\alpha}_n x}\left[\sin\delta_n(y+b) + \frac{i\zeta}{k}\delta_n\cos\delta_n(y+b)\right]. \tag{2.16}$$

In region $(-a \leq y \leq a,\ x < 0)$ the acoustic wave shows incident and reflected behavior while in the regions $(-b \leq y \leq -a,\ x < 0)$ and $(a \leq y \leq b,\ x < 0)$ transmission behavior is observed. In the text R_n and T_n represent reflection and transmission coefficients, respectively. To arrive at a unique solution, we also require the "edge conditions" [18]

$$\Phi(x, \pm a) = O(1), \quad \Phi_y(x, \pm a) = O\left(x^{-1/2}\right) \quad \text{as } x \longrightarrow 0. \tag{2.17}$$

3. The Wiener-Hopf (WH) Equations

For analytic convenience, we will assume that $k = k_1 + ik_2$ $(k_1 > 0,\ k_2 \geq 0)$ since the time dependence is taken to be of the form $e^{-i\omega t}$ [15]. Let us define Fourier transform and its inverse by

$$\widehat{\Phi}(\alpha, y) = \int_{-\infty}^{\infty} \Phi(x, y) e^{i\alpha x} dx = \widehat{\Phi}_+(\alpha, y) + \widehat{\Phi}_-(\alpha, y), \tag{3.1}$$

$$\Phi(x, y) = \frac{1}{2\pi} \int_{-\infty}^{\infty} \widehat{\Phi}(\alpha, y) e^{-i\alpha x} d\alpha. \tag{3.2}$$

In (3.1),

$$\begin{aligned} \widehat{\Phi}_+(\alpha, y) &= \int_{0}^{\infty} \Phi(x, y) e^{i\alpha x} dx, \\ \widehat{\Phi}_-(\alpha, y) &= \int_{-\infty}^{0} \Phi(x, y) e^{i\alpha x} dx, \end{aligned} \tag{3.3}$$

where α is a complex variable with

$$\alpha = \sigma + i\tau. \tag{3.4}$$

Use of (3.1) to (2.3) gives

$$\frac{d^2\widehat{\Phi}}{dy^2} + \kappa^2 \widehat{\Phi} = 0, \tag{3.5}$$

where

$$\kappa(\alpha) = \sqrt{k^2 - \alpha^2}. \tag{3.6}$$

The suitable solutions of (3.5) in the trifurcated regions are

$$\widehat{\Phi}(\alpha, y) = A_1(\alpha) \cos \kappa y + B_1(\alpha) \sin \kappa y \quad (-b \leq y \leq -a), \tag{3.7}$$

$$\widehat{\Phi}(\alpha, y) = \frac{-i}{\alpha + \chi_1} \sin\left[\frac{\pi(y - a)}{2a}\right] + A_2(\alpha) \cos \kappa y + B_2(\alpha) \sin \kappa y \quad (-a \leq y \leq a), \tag{3.8}$$

$$\widehat{\Phi}(\alpha, y) = A_3(\alpha) \cos \kappa y + B_3(\alpha) \sin \kappa y \quad (a \leq y \leq b), \tag{3.9}$$

where the first term on the right-hand side of (3.8) comes from the incident field. On taking Fourier transform, (2.4)–(2.9) become

$$\widehat{\Phi}(\alpha, b) + \left(\frac{i\zeta}{k}\right)\widehat{\Phi}'(\alpha, b) = 0, \tag{3.10}$$

$$\widehat{\Phi}_{-}(\alpha, a) = 0, \tag{3.11}$$

$$\widehat{\Phi}_{-}(\alpha, -a) = 0, \tag{3.12}$$

$$\widehat{\Phi}(\alpha, -b) - \left(\frac{i\zeta}{k}\right)\widehat{\Phi}'(\alpha, -b) = 0, \tag{3.13}$$

$$\widehat{\Phi}'_{+}(\alpha, -a^{+}) = \widehat{\Phi}'_{+}(\alpha, -a^{-}), \tag{3.14}$$

$$\widehat{\Phi}'_{+}(\alpha, a^{+}) = \widehat{\Phi}'_{+}(\alpha, a^{-}), \tag{3.15}$$

where prime denotes the differentiation with respect to y. In order to determine the unknowns $A_j(\alpha)$ and $B_j(\alpha)$ ($j = 1$, 2 and 3), we proceed to satisfy boundary conditions (3.10)–(3.13). Thus, by invoking (3.12) and (3.13) in (3.7), we may write

$$\begin{gathered} A_1(\alpha)\cos\kappa a - B_1(\alpha)\sin\kappa a = \Phi_1^{+}(\alpha), \\ A_1(\alpha)\left(\cos\kappa b - \left(\frac{i\zeta}{k}\right)\kappa\sin\kappa b\right) - B_1(\alpha)\left(\sin\kappa b + \left(\frac{i\zeta}{k}\right)\kappa\cos\kappa b\right) = 0, \end{gathered} \tag{3.16}$$

where $\Phi_1^{+}(\alpha) = \widehat{\Phi}_{+}(\alpha, -a)$ is analytic in $\operatorname{Im}\alpha > -\operatorname{Im}k$. Solving, above equations for $A_1(\alpha)$ and $B_1(\alpha)$ we obtain

$$\begin{aligned} A_1(\alpha) &= \frac{\sin\kappa b + (i\zeta/k)\kappa\cos\kappa b}{\sin\kappa(b-a) + (i\zeta/k)\kappa\cos\kappa(b-a)}\Phi_1^{+}(\alpha), \\ B_1(\alpha) &= \frac{\cos\kappa b - (i\zeta/k)\kappa\sin\kappa b}{\sin\kappa(b-a) + (i\zeta/k)\kappa\cos\kappa(b-a)}\Phi_1^{+}(\alpha). \end{aligned} \tag{3.17}$$

Again, using (3.11) and (3.12) in (3.8), we may write

$$\begin{gathered} A_2(\alpha)\cos\kappa a + B_2(\alpha)\sin\kappa a = \Phi_2^{+}(\alpha), \\ A_2(\alpha)\cos\kappa a - B_2(\alpha)\sin\kappa a = \Phi_1^{+}(\alpha), \end{gathered} \tag{3.18}$$

where $\Phi_2^{+}(\alpha) = \widehat{\Phi}_{+}(\alpha, a)$ is analytic in $\operatorname{Im}\alpha > -\operatorname{Im}k$. Solving (3.18) for $A_2(\alpha)$ and $B_2(\alpha)$, we obtain

$$\begin{aligned} A_2(\alpha) &= \frac{\sin\kappa a\left(\Phi_1^{+}(\alpha) + \Phi_2^{+}(\alpha)\right)}{\sin 2\kappa a}, \\ B_2(\alpha) &= \frac{\cos\kappa a\left(\Phi_2^{+}(\alpha) - \Phi_1^{+}(\alpha)\right)}{\sin 2\kappa a}. \end{aligned} \tag{3.19}$$

With the use of (3.10) and (3.11) in (3.9), we may write

$$A_3(\alpha)\left(\cos\kappa b-\left(\frac{i\zeta}{k}\right)\kappa\sin\kappa b\right)+B_3(\alpha)\left(\sin\kappa b+\left(\frac{i\zeta}{k}\right)\kappa\cos\kappa b\right)=0,$$
$$A_3(\alpha)\cos\kappa a+B_3(\alpha)\sin\kappa a=\Phi_2^+(\alpha). \tag{3.20}$$

Solving for $A_3(\alpha)$ and $B_3(\alpha)$, we obtain

$$A_3(\alpha)=\frac{\sin\kappa b+(i\zeta/k)\kappa\cos\kappa b}{\sin\kappa(b-a)+(i\zeta/k)\kappa\cos\kappa(b-a)}\Phi_2^+(\alpha),$$
$$B_3(\alpha)=-\frac{\cos\kappa b-(i\zeta/k)\kappa\sin\kappa b}{\sin\kappa(b-a)+(i\zeta/k)\kappa\cos\kappa(b-a)}\Phi_2^+(\alpha). \tag{3.21}$$

By substituting the above values of $A_j(\alpha)$ and $B_j(\alpha)$ $(j=1,\ 2$ and $3)$ in (3.7)–(3.9) we get

$$\widehat{\Phi}(\alpha,y)=\frac{\sin\kappa(y+b)+(i\zeta/k)\kappa\cos\kappa(y+b)}{\sin\kappa(b-a)+(i\zeta/k)\kappa\cos\kappa(b-a)}\Phi_1^+(\alpha)\quad(-b\le y\le -a),$$
$$\widehat{\Phi}(\alpha,y)=\frac{-i}{\alpha+\chi_1}\sin\left[\frac{\pi(y-a)}{2a}\right]$$
$$+\frac{1}{\sin 2\kappa a}\left(\Phi_2^+(\alpha)\sin\kappa(y+a)-\Phi_1^+(\alpha)\sin\kappa(y-a)\right)\quad(-a\le y\le a), \tag{3.22}$$
$$\widehat{\Phi}(\alpha,y)=\frac{\sin\kappa(b-y)+(i\zeta/k)\kappa\cos\kappa(y-b)}{\sin\kappa(b-a)+(i\zeta/k)\kappa\cos\kappa(b-a)}\Phi_2^+(\alpha)\quad(a\le y\le b).$$

Invoking (3.22) in (3.14) and (3.15), we arrive at

$$\frac{-\kappa(\sin\kappa(b+a)+(i\zeta/k)\kappa\cos\kappa(b+a))\Phi_1^+(\alpha)}{\sin 2\kappa a(\sin\kappa(b-a)+(i\zeta/k)\kappa\cos\kappa(b-a))}+\frac{\kappa\Phi_2^+(\alpha)}{\sin 2\kappa a}-\frac{\lambda_1}{\alpha+\chi_1}=\Phi_1^-(\alpha),$$
$$\frac{\kappa(\sin\kappa(b+a)+(i\zeta/k)\kappa\cos\kappa(b+a))\Phi_2^+(\alpha)}{\sin 2\kappa a(\sin\kappa(b-a)+(i\zeta/k)\kappa\cos\kappa(b-a))}-\frac{\kappa\Phi_1^+(\alpha)}{\sin 2\kappa a}+\frac{\lambda_1}{\alpha+\chi_1}=\Phi_2^-(\alpha), \tag{3.23}$$

where

$$\lambda_1=\frac{-i\pi}{2a},$$
$$\Phi_1^-(\alpha)=\widehat{\Phi}'_-(\alpha,-a^-)-\widehat{\Phi}'_-(\alpha,-a^+), \tag{3.24}$$
$$\Phi_2^-(\alpha)=\widehat{\Phi}'_-(\alpha,a^-)-\widehat{\Phi}'_-(\alpha,a^+).$$

The functions $\Phi_1^-(\alpha)$ and $\Phi_2^-(\alpha)$ are analytic in the region $\operatorname{Im}\alpha < \operatorname{Im}k$. Addition and subtraction of (3.23) will give

$$\begin{gathered} W(\alpha)D_+(\alpha) = S_-(\alpha), \\ K(\alpha)S_+(\alpha) + \frac{2\lambda_1}{\alpha+\chi_1} = D_-(\alpha), \end{gathered} \tag{3.25}$$

where

$$\Phi_2^{\pm}(\alpha) - \Phi_1^{\pm}(\alpha) = D_{\pm}(\alpha), \tag{3.26}$$

$$\Phi_2^{\pm}(\alpha) + \Phi_1^{\pm}(\alpha) = S_{\pm}(\alpha), \tag{3.27}$$

$$K(\alpha) = \frac{\kappa(\cos\kappa b - (i\zeta/k)\kappa\sin\kappa b)}{\cos\kappa a(\sin\kappa(b-a) + (i\zeta/k)\kappa\cos\kappa(b-a))}, \tag{3.28}$$

$$W(\alpha) = \frac{\kappa(\sin\kappa b + (i\zeta/k)\kappa\cos\kappa b)}{\sin\kappa a(\sin\kappa(b-a) + (i\zeta/k)\kappa\cos\kappa(b-a))}. \tag{3.29}$$

4. Solution of the Problem

Writing (see the appendix)

$$W(\alpha) = W_+(\alpha)W_-(\alpha), \quad K(\alpha) = K_+(\alpha)K_-(\alpha), \tag{4.1}$$

where $(+)$ is the subscript assigned to the function regular in the upper half plane $\operatorname{Im}\alpha > -\operatorname{Im}k$ and the subscript $(-)$ represents the function regular in the lower half plane $\operatorname{Im}\alpha < \operatorname{Im}k$. Now from (3.25), we have

$$\begin{gathered} W_+(\alpha)D_+(\alpha) = \frac{S_-(\alpha)}{W_-(\alpha)}, \\ K_+(\alpha)S_+(\alpha) + \frac{2\lambda_1}{(\alpha+\chi_1)K_-(-\chi_1)} = \frac{D_-(\alpha)}{K_-(\alpha)} - \frac{2\lambda_1}{\alpha+\chi_1}\left[\frac{1}{K_-(\alpha)} - \frac{1}{K_-(-\chi_1)}\right]. \end{gathered} \tag{4.2}$$

Note that the left-hand side of both equations is analytic in $\operatorname{Im}\alpha > -\operatorname{Im}k$ and the right-hand side is analytic in $\operatorname{Im}\alpha < \operatorname{Im}k$. Also, when $|\alpha| \to \infty$,

$$\begin{gathered} K_{\pm}(\alpha) = O\left(|\alpha|^{1/2}\right), \\ W_{\pm}(\alpha) = O\left(|\alpha|^{1/2}\right), \end{gathered} \tag{4.3}$$

and Fourier transform of edge conditions (2.17) helps us to determine the asymptotic behavior of $D_{\pm}(\alpha)$ and $S_{\pm}(\alpha)$. For $|\alpha| \to \infty$,

$$\begin{aligned} D_{-}(\alpha) &= O\left(|\alpha|^{-1}\right), \quad S_{-}(\alpha) = O\left(\alpha^{-1}\right) \quad \text{for } \operatorname{Im}\alpha < \operatorname{Im}k, \\ D_{+}(\alpha) &= O\left(|\alpha|^{-1}\right), \quad S_{+}(\alpha) = O\left(\alpha^{-1/2}\right) \quad \text{for } \operatorname{Im}\alpha > -\operatorname{Im}k. \end{aligned} \tag{4.4}$$

Now the use of (4.3)–(4.4) and standard Wiener-Hopf procedure [15] on (4.2) give

$$\begin{aligned} D_{+}(\alpha) &= 0, \\ K_{+}(\alpha)S_{+}(\alpha) + \frac{2\lambda_1}{(\alpha+\chi_1)K_{+}(\chi_1)} &= 0, \end{aligned} \tag{4.5}$$

where $K_{-}(-\chi_1) = K_{+}(\chi_1)$. Using (3.26) and (3.27) in (4.5), we get

$$\begin{aligned} \Phi_1^{+}(\alpha) &= -\frac{\lambda_1}{(\alpha+\chi_1)K_{+}(\alpha)K_{+}(\chi_1)}, \\ \Phi_2^{+}(\alpha) &= -\frac{\lambda_1}{(\alpha+\chi_1)K_{+}(\alpha)K_{+}(\chi_1)}. \end{aligned} \tag{4.6}$$

From (3.22) and (4.6), we obtain the field representations for the different regions as follows.

When $(-b \le y \le -a)$,

$$\widehat{\Phi}(\alpha, y) = -\frac{\lambda_1}{\sin\kappa(b-a) + (i\zeta/k)\kappa\cos\kappa(b-a)}\left\{\frac{\sin\kappa(y+b) + (i\zeta/k)\kappa\cos\kappa(y+b)}{(\alpha+\chi_1)K_{+}(\alpha)K_{+}(\chi_1)}\right\}. \tag{4.7}$$

For $(-a \le y \le a)$, one obtains

$$\widehat{\Phi}(\alpha, y) = \frac{-i}{\alpha+\chi_1}\sin\left[\frac{\pi(y-a)}{2a}\right] - \frac{\lambda_1}{\cos\kappa a}\left\{\frac{\cos\kappa y}{(\alpha+\chi_1)K_{+}(\alpha)K_{+}(\chi_1)}\right\}. \tag{4.8}$$

For $(a \le y \le b)$, one has

$$\widehat{\Phi}(\alpha, y) = -\frac{\lambda_1}{\sin\kappa(b-a) + (i\zeta/k)\kappa\cos\kappa(b-a)}\left\{\frac{\sin\kappa(b-y) + (i\zeta/k)\kappa\cos\kappa(y-b)}{(\alpha+\chi_1)K_{+}(\alpha)K_{+}(\chi_1)}\right\}. \tag{4.9}$$

Taking inverse Fourier transform of (4.7)–(4.9), we obtain the following.

For the region $(-b \le y \le -a,\ x < 0)$, one may write

$$\Phi(x,y) = -\frac{\lambda_1}{2\pi}\int_{-\infty+i\tau}^{\infty+i\tau} \frac{e^{-i\alpha x}}{\sin\kappa(b-a) + (i\zeta/k)\kappa\cos\kappa(b-a)} \times \left\{\frac{\sin\kappa(y+b) + (i\zeta/k)\kappa\cos\kappa(y+b)}{(\alpha+\chi_1)K_+(\alpha)K_+(\chi_1)}\right\} d\alpha. \tag{4.10}$$

When $(-a \le y \le a,\ x < 0)$, we have

$$\Phi(x,y) = e^{i\chi_1 x}\sin\left[\frac{\pi(y-a)}{2a}\right] - \frac{\lambda_1}{2\pi}\int_{-\infty+i\tau}^{\infty+i\tau} \frac{e^{-i\alpha x}}{\cos\kappa a}\left\{\frac{\cos\kappa y}{(\alpha+\chi_1)K_+(\alpha)K_+(\chi_1)}\right\} d\alpha. \tag{4.11}$$

For $(a \le y \le b,\ x < 0)$, we arrive at

$$\Phi(x,y) = \frac{\lambda_1}{2\pi}\int_{-\infty+i\tau}^{\infty+i\tau} \frac{e^{-i\alpha x}}{\sin\kappa(b-a) + (i\zeta/k)\kappa\cos\kappa(b-a)} \times \left\{\frac{\sin\kappa(y-b) - (i\zeta/k)\kappa\cos\kappa(y-b)}{(\alpha+\chi_1)K_+(\alpha)K_+(\chi_1)}\right\} d\alpha. \tag{4.12}$$

For $(-b \le y \le b,\ x > 0)$, one may write

$$\Phi(x,y) = \frac{\lambda_1}{2\pi}\int_{-\infty+i\tau}^{\infty+i\tau} \frac{e^{-i\alpha x}}{\cos\kappa b - (i\zeta/k)\kappa\sin\kappa b} \times \left\{\frac{(\sin\kappa(y-b) - (i\zeta/k)\kappa\cos\kappa(y-b))\cos\kappa a K_-(\alpha)}{\kappa(\alpha+\chi_1)K_+(\chi_1)}\right\} d\alpha. \tag{4.13}$$

In (4.10)–(4.13), τ is the imaginary part of α, $\kappa(\alpha) = \sqrt{k^2-\alpha^2}$ and branch cuts are taken to be from k to $i\infty$ and $-k$ to $-i\infty$, and $0 \le \arg\kappa \le \pi$ (Figure 2). Note that the integrands have no singularities which lie on the contour of integration. To evaluate the integrals in (4.10)–(4.13), it is noted that the contour of integration in these equations lies in the strip $-\operatorname{Im}k < \operatorname{Im}\alpha < \operatorname{Im}k$.

In expressions (4.10)–(4.13), the pole $\alpha = -\chi_1$ lies below the contour of integration. One can also note that the terms in the curly brackets $\{\ \}$ of (4.10)–(4.12) have no branch points in $\operatorname{Im}\alpha > -\operatorname{Im}k$ and those in (4.13) have no branch points in $\operatorname{Im}\alpha < \operatorname{Im}k$. Thus the only singularities in the integrands of (4.10) and (4.12) occur at the zeros of

$$\sin\kappa(b-a) + \left(\frac{i\zeta}{k}\right)\kappa\cos\kappa(b-a) = 0, \tag{4.14}$$

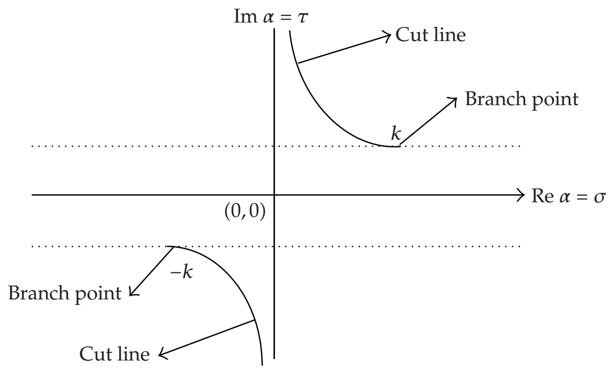

Figure 2: Strip of analyticity and branch cuts in the complex α-plane.

that is, at

$$\alpha = \widetilde{\alpha}_n = \left(k^2 - \delta_n^2\right)^{1/2} \quad (n = 1, 2, 3, \ldots). \tag{4.15}$$

The only singularities of (4.11) occur at the zeros of $\cos \kappa a = 0$, that is at

$$\alpha = \widetilde{\chi}_{2n-1} = \left(k^2 - \frac{(2n-1)^2 \pi^2}{4a^2}\right)^{1/2} \quad (n = 1, 2, 3, \ldots). \tag{4.16}$$

The only singularities in the integrands in (4.13) occur at the zeros of

$$\cos \kappa b - \left(\frac{i\zeta}{k}\right) \kappa \sin \kappa b = 0, \tag{4.17}$$

that is at

$$\alpha = -\sigma_n = -\left(k^2 - \beta_n^2\right)^{1/2} \quad (n = 1, 2, 3, \ldots). \tag{4.18}$$

5. Modal Field Representation

Invoking Cauchy residue theorem [17] to the integrals in (4.10)–(4.13), we obtain the following.

When $(-b \le y \le -a,\ x < 0)$,

$$\Phi(x, y) = -\sum_{n=1}^{\infty} \frac{e^{-i\widetilde{\alpha}_n x}}{q_1'(\widetilde{\alpha}_n)} \left\{ \frac{(\sin \delta_n (y + b) + (i\zeta/k) \delta_n \cos \delta_n (y + b))\pi}{2a(\widetilde{\alpha}_n + \chi_1) K_+(\widetilde{\alpha}_n) K_+(\chi_1)} \right\}, \tag{5.1}$$

where

$$q_1(\alpha) = \sin\kappa(b-a) + \left(\frac{i\zeta}{k}\right)\kappa\cos\kappa(b-a),$$
$$\tilde{\alpha}_n = \left(k^2 - \delta_n^2\right)^{1/2} \quad (n = 1,2,3,\ldots). \tag{5.2}$$

For $(-a \le y \le a,\ x < 0)$, we have

$$\Phi(x,y) = e^{i\chi_1 x}\sin\left[\frac{\pi(y-a)}{2a}\right] - \sum_{n=1}^{\infty}\frac{\pi\alpha_{2n-1}(-1)^{n+1}e^{-i\chi_{2n-1}x}\cos(\alpha_{2n-1}y)}{2a^2\chi_{2n-1}(\chi_{2n-1}+\chi_1)K_+(\chi_{2n-1})K_+(\chi_1)}. \tag{5.3}$$

For $(a \le y \le b,\ x < 0)$, we arrive at

$$\Phi(x,y) = \sum_{n=1}^{\infty}\frac{e^{-i\tilde{\alpha}_n x}}{q_1'(\tilde{\alpha}_n)}\left\{\frac{(\sin\delta_n(y-b) - (i\zeta/k)\delta_n\cos\delta_n(y-b))\pi}{2a(\tilde{\alpha}_n+\chi_1)K_+(\tilde{\alpha}_n)K_+(\chi_1)}\right\}. \tag{5.4}$$

When $(-b \le y \le b,\ x > 0)$, we have

$$\Phi(x,y) = \sum_{n=1}^{\infty}\frac{e^{i\sigma_n x}(\sin\beta_n(y-b) - (i\zeta/k)\beta_n\cos\beta_n(b-y))\pi\cos\beta_n a}{2am'(-\sigma_n)K_+(\chi_1)(\chi_1-\sigma_n)\beta_n}K_-(-\sigma_n), \tag{5.5}$$

where

$$m(\alpha) = \cos\kappa b - \left(\frac{i\zeta}{k}\right)\kappa\sin\kappa b,$$
$$\alpha = -\sigma_n = -\left(k^2 - \beta_n^2\right)^{1/2} \quad (n = 1,2,3,\ldots). \tag{5.6}$$

6. Reflection Coefficient

Inside the waveguide field intensity is superposition of reflected and transmitted waves. Hence, it is relevant to deal with reflection or transmission coefficients which are related to relative energy. We will consider reflection coefficient for the first mode $n = 1$ given by (5.3) as

$$R_1 = \frac{\pi^2}{8a^3\chi_1^2(K_+(\chi_1))^2}. \tag{6.1}$$

7. Numerical and Graphical Results

The expression of field intensity involves infinite sums/products for which we have used numerical technique and obtained the results using truncation approach [19]. We have

Table 1: Field intensity $|\Phi|$ versus the truncation number n for different boundary conditions of the semi-infinite duct.

n	$a = 0.5, b = 3a, k = 0.5, y = 1, \xi = 1.5, \eta = 1$ and $x = -0.1$	
	$\|\Phi\|$ for hard boundary conditions	$\|\Phi\|$ for soft boundary conditions
10	1.809170	0.824323
20	1.853300	0.878547
30	1.883790	0.899716
40	1.905980	0.911027
50	1.922750	0.918070
60	1.935870	0.922877
70	1.946400	0.926369
80	1.955050	0.929019
90	1.962260	0.931100
100	1.968380	0.932777
110	1.973630	0.934157
120	1.978180	0.935313
130	1.982170	0.936295
140	1.985700	0.937140
150	1.988830	0.937874

computed the results of variation of field intensity for different boundary conditions of the semi-infinite duct at n from 10 to 150 by step 10 given in Table 1. From this table, it is evident that the presence of soft boundary condition induces a good noise reduction as compared with hard boundary conditions.

The values of specific impedance $\zeta = \xi + i\eta$ $(= z/\rho_0 c)$ for an absorbing sheet which seem to have practical importance are [13]

fibrous sheet: $\xi = 0.5, -1 < \eta < 3$,

perforated sheet: $0 < \xi < 3, -1 < \eta < 3$.

The convergence of the field can be checked through the relative error for which the suitable definition would be

$$E_n = \max_{x,y} \frac{|\Phi_n(x,y) - \Phi_N(x,y)|}{|\Phi_N(x,y)|}, \tag{7.1}$$

where $\Phi_n(x,y)$ is the solution obtained using the truncation number n and N is suitably large truncation number ($N = 150$).

For a comprehensive numerical study, we need a considerable number of graphs because of the number of parameters which determine the diffracted field. The computer programme "MATHEMATICA 5.2" is used for the numerical evaluation and graphical representation of the functions given by (6.1) and (7.1).

In Figures 3 and 4, the field intensity is plotted against the wave number k for different values of noise reduction parameters, that is, ξ (real part of ζ) and η (the imaginary part of ζ).

In Figure 5, the reflected field is plotted against wave number k for different values of b (separation distance between the infinite plates). In Figure 6, variation of relative error E_n against truncation number n is plotted.

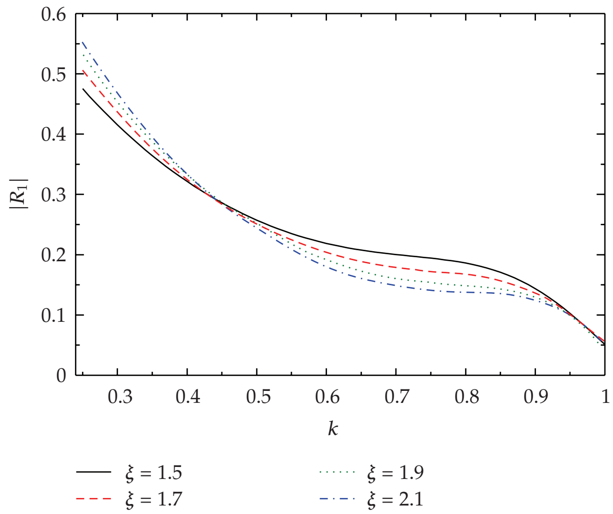

Figure 3: Variation of field intensity $|R_1|$ with wave number k for several values of ξ corresponding to $\eta = 0.5$, $a = 1$, and $b = 3a$.

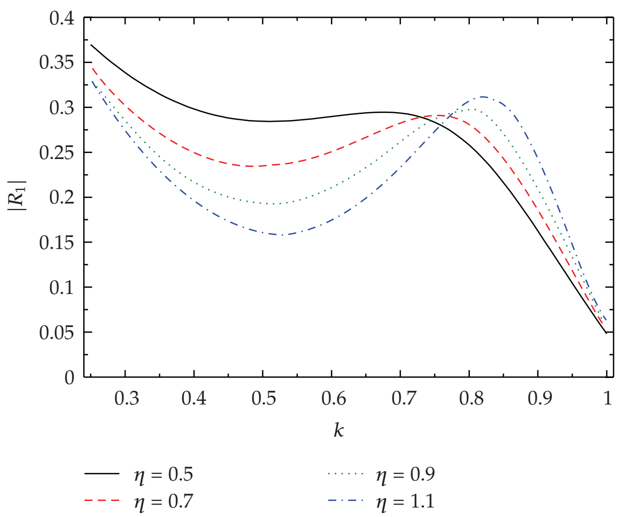

Figure 4: Variation of field intensity $|R_1|$ with wave number k for several values of η corresponding to $\xi = 1$, $a = 1$, and $b = 3a$.

The main findings from the analysis are summarized in the following points.

(i) Global speaking, it is noted that the reflected field is a decreasing function of the real and imaginary parts of the absorbing parameter but with relative or local maxima and minima.

(ii) Gradually increase in the separation distance between the infinite plates yields a decrease in the value of reflected field intensity.

(iii) The absolute values of the reflection coefficient are in accordance with the conservation of energy rules.

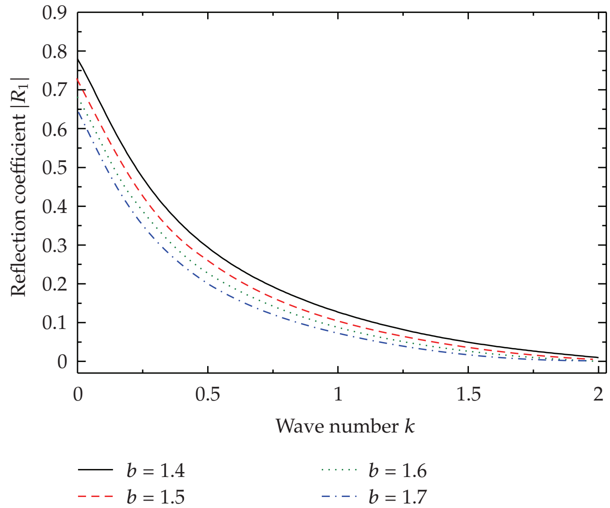

Figure 5: Variation of $|R_1|$ with k for several values of b corresponding to $\eta = 1$, $\xi = 2.50$, and $a = b/2$.

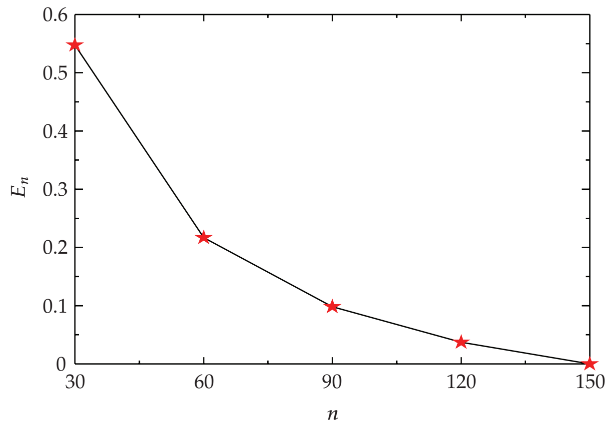

Figure 6: Variation of relative error E_n with truncation number n corresponding to $a = 0.5$, $b = 3a$, $x = -0.1$, $k = 0.7$, $y = 1$, $\xi = 0.5$, and $\eta = 1$.

(iv) The findings confirm that the relative error reduces by increasing the truncation number n.

(v) The established results clearly show the contribution that arises because of the soft surfaces.

8. Final Remarks

Computation of acoustic diffraction is very important in the analysis of acoustic waveguide systems. In this study the Wiener-Hopf method has been used for diffraction of acoustic waves in a trifurcated waveguide. The problem consists of absorbing and soft surfaces. A sound wave of first mode propagating out of the mouth of the semi-infinite soft duct is taken into account. The problem is formulated first and then solved analytically. For the quality of the computation, the comparison of the hard [13] with the soft boundary conditions of the semi-infinite duct is discussed in detail. To enhance the quality of the results some graphs are plotted for sundry parameters of interest using wave number versus reflection coefficient of first mode in absolute value. It is observed that soft surfaces show good noise reduction effects on the noise transmitted through the waveguide as compared with hard surfaces [13]. This is a canonical problem of mathematical interest. The reported results are shown conclusively and present a comprehensive introduction on the current state of art within the field of guide acoustics.

Appendix

The main purpose of this appendix is to give the complete factorization of the kernel functions $K(\alpha)$ and $W(\alpha)$ and to show their asymptotic behavior as $|\alpha| \to \infty$. The factorization of these functions $K(\alpha)$ and $W(\alpha)$ is of the form

$$K(\alpha) = K_+(\alpha)K_-(\alpha), \qquad W(\alpha) = W_+(\alpha)W_-(\alpha), \tag{A.1}$$

where $K_+(\alpha)$ and $W_+(\alpha)$ denote certain functions which are regular and free of zeros in upper half plane $\operatorname{Im}\alpha > -\operatorname{Im}k$ and $K_-(\alpha)$ and $W_-(\alpha)$ denote certain functions which are regular and free of zeros in lower half plane $\operatorname{Im}\alpha < \operatorname{Im}k$.

We may note that the functions $K(\alpha)$ and $W(\alpha)$ are even in Fourier transform parameter α and more precisely their respective derivatives are zero at $\alpha = 0$. So these functions can be factorized by applying the infinite product expansion of an integral function with infinitely many zeros [15, 20]. For given $K(\alpha)$ by (3.28), we have

$$K(\alpha) = \frac{\kappa(\cos\kappa b - (i\zeta/k)\kappa\sin\kappa b)}{\cos\kappa a(\sin\kappa(b-a) + (i\zeta/k)\kappa\cos\kappa(b-a))}. \tag{A.2}$$

It is evident that the product factorization of $K(\alpha)$ depends upon the factorization of

$$\begin{aligned} L(\alpha) &= \cos\kappa b - \left(\frac{i\zeta}{k}\right)\kappa\sin\kappa b, \\ N(\alpha) &= \frac{\sin\kappa(b-a)}{\kappa} + \left(\frac{i\zeta}{k}\right)\cos\kappa(b-a), \\ P(\alpha) &= \cos\kappa a. \end{aligned} \tag{A.3}$$

By employing the procedure outlined by Mittra and Lee [21], we have

$$L_+(\alpha) = \sqrt{\cos kb - i\zeta\sin kb}\exp\left\{\frac{i\alpha b}{\pi}\left[1 - C - \ln\left(\frac{|\alpha| b}{\pi}\right) + \frac{i\pi}{2}\right]\right\}\prod_{n=1}^{\infty}\left(1 + \frac{\alpha}{\sigma_n}\right)\exp\left(\frac{i\alpha b}{n\pi}\right),$$

$$N_+(\alpha) = \sqrt{\frac{\sin k(b-a)}{k} + \left(\frac{i\zeta}{k}\right)\cos k(b-a)}\exp\left\{\frac{i\alpha(b-a)}{\pi}\left[1 - C - \ln\left(\frac{|\alpha|(b-a)}{\pi}\right) + \frac{i\pi}{2}\right]\right\}$$
$$\times \prod_{n=1}^{\infty}\left(1 + \frac{\alpha}{\widetilde{\alpha}_n}\right)\exp\left(\frac{i\alpha(b-a)}{n\pi}\right),$$
$$P_+(\alpha) = \sqrt{\cos ka}\exp\left\{\frac{i2\alpha a}{\pi}\left[1 - C - \ln\left(\frac{|\alpha|2a}{\pi}\right) + \frac{i\pi}{2}\right]\right\}\prod_{n=1}^{\infty}\left(1 + \frac{\alpha}{\widetilde{\chi}_{2n-1}}\right)\exp\left(\frac{i2\alpha a}{(2n-1)\pi}\right), \tag{A.4}$$

with

$$K_+(\alpha) = \frac{L_+(\alpha)}{N_+(\alpha)P_+(\alpha)}. \tag{A.5}$$

Thus

$$K(\alpha) = K_+(\alpha)K_-(\alpha), \tag{A.6}$$

where

$$\begin{aligned} K_+(\alpha) = {} & \sqrt{\frac{k(\cos kb - i\zeta\sin kb)}{\cos ka(\sin k(b-a) + i\zeta\cos k(b-a))}} \\ & \times \frac{\exp\{(i\alpha b/\pi)[1 - C - \ln(|\alpha|b/\pi) + i\pi/2]\}}{\exp\{(i2\alpha a/\pi)[1 - C - \ln(|\alpha|2a/\pi) + i\pi/2]\}} \\ & \times \frac{1}{\exp\{(i\alpha(b-a)/\pi)[1 - C - \ln(|\alpha|(b-a)/\pi) + i\pi/2]\}} \\ & \times \prod_{n=1}^{\infty}\frac{(1 + \alpha/\sigma_n)\exp(i\alpha b/n\pi)}{(1 + \alpha/\widetilde{\chi}_{2n-1})\exp(i2\alpha a/((2n-1)\pi))(1 + \alpha/\widetilde{\alpha}_n)\exp(i\alpha(b-a)/n\pi)}. \end{aligned} \tag{A.7}$$

Here $\sigma_n' s$, $\widetilde{\alpha}_n' s$ and $\widetilde{\chi}_{2n-1}' s$ are the roots of the functions $L(\alpha)$, $N(\alpha)$, and $P(\alpha)$, respectively,

$$L(\sigma_n) = 0, \quad N(\widetilde{\alpha}_n) = 0, \quad P(\widetilde{\chi}_{2n-1}) = 0, \quad n = 1, 2, 3, \ldots. \tag{A.8}$$

with

$$L_-(\alpha) = L_+(-\alpha), \qquad N_-(\alpha) = N_+(-\alpha), \qquad P_-(\alpha) = P_+(-\alpha) \tag{A.9}$$

and C being Euler's constant given by $C = 0.57721\ldots$ and $K_+(\alpha) = K_-(-\alpha)$. In the respective region of analyticity, when $|\alpha| \to \infty$,

$$K_\pm(\alpha) = O\left(|\alpha|^{1/2}\right). \tag{A.10}$$

Similarly, for $W(\alpha)$ given by (3.29),

$$W(\alpha) = \frac{\kappa(\sin\kappa b + (i\zeta/k)\kappa\cos\kappa b)}{\sin\kappa a(\sin\kappa(b-a) + (i\zeta/k)\kappa\cos\kappa(b-a))}. \tag{A.11}$$

By following the above procedure [21], we can write

$$\begin{aligned} W_+(\alpha) = {}& \sqrt{\frac{k(\sin kb + i\zeta\cos kb)}{\sin ka(\sin k(b-a) + i\zeta\cos k(b-a))}} \\ & \times \frac{\exp\{(i\alpha b/\pi)[1 - C - \ln(|\alpha|b/\pi) + i\pi/2]\}}{\exp\{(i\alpha a/\pi)[1 - C - \ln(|\alpha|a/\pi) + i\pi/2]\}} \\ & \times \frac{1}{\exp\{(i\alpha(b-a)/\pi)[1 - C - \ln(|\alpha|(b-a)/\pi) + i\pi/2]\}} \\ & \times \prod_{n=1}^{\infty} \frac{(1+\alpha/\tilde{\sigma}_n)\exp(i\alpha b/n\pi)}{(1+\alpha/\widehat{\sigma}_n)\exp(i\alpha a/n\pi)(1+\alpha/\tilde{\alpha}_n)\exp(i\alpha(b-a)/n\pi)}, \end{aligned} \tag{A.12}$$

with

$$W_+(\alpha) = W_-(-\alpha). \tag{A.13}$$

Also, when $|\alpha| \to \infty$, in the respective region of analyticity,

$$W_\pm(\alpha) = O\left(|\alpha|^{1/2}\right). \tag{A.14}$$

References

[1] A. D. Rawlins, "Radiation of sound from an unflanged rigid cylindrical duct with an acoustically absorbing internal surface," *Proceedings of the Royal Society London Series A*, vol. 361, no. 1704, pp. 65–91, 1978.

[2] A. Demir and A. Büyükaksoy, "Radiation of plane sound waves by a rigid circular cylin- drical pipe with a partial internal impedance loading," *Acta Acustica united with Acustica*, vol. 89, pp. 578–585, 2003.

[3] W. Koch, "Attenuation of sound in multi-element acoustically lined rectangular ducts in the absence of mean flow," *Journal of Sound and Vibration*, vol. 52, no. 4, pp. 459–496, 1977.

[4] W. Koch, "Radiation of sound from a two-dimensional acoustically lined duct," *Journal of Sound and Vibration*, vol. 55, no. 2, pp. 255–274, 1977.

[5] D. S. Jones, "Diffraction by three semi-infinite planes," *Proceedings of the Royal Society London Series A*, vol. 404, no. 1827, pp. 299–321, 1986.

[6] S. Asghar, M. Ayub, and B. Ahmad, "Point source diffraction by three half planes in a moving fluid," *Wave Motion*, vol. 15, no. 3, pp. 201–220, 1992.

[7] M. Hassan and A. D. Rawlins, "Radiation from a two dimensional duct," *Canadian Journal of Physics*, vol. 1, pp. 375–384, 1997.

[8] S. Asghar and T. Hayat, "Scattering in an absorbing parallel plate system," *Acoustics Letters*, vol. 20, no. 9, pp. 185–190, 1997.

[9] A. Snakowska, "Diffraction of sound waves at the opening of a soft cylindrical duct," *European Physical Journal-Special Topics*, vol. 154, pp. 201–205, 2008.

[10] A. Büyükaksoy and B. Polat, "A bifurcated waveguide problem," *Bulletin of the Technical University of Istanbul*, vol. 51, no. 3, pp. 196–202, 1999.

[11] A. D. Rawlins, "Two waveguide trifurcation problems," *Mathematical Proceedings of the Cambridge Philosophical Society*, vol. 121, no. 3, pp. 555–573, 1997.

[12] M. Ayub, M. H. Tiwana, and A. B. Mann, "Propagation of sound in a duct with mean flow," *Communications in Nonlinear Science and Numerical Simulation*, vol. 14, no. 9-10, pp. 3578–3590, 2009.

[13] M. Hassan and A. D. Rawlins, "Sound radiation in a planar trifurcated lined duct," *Wave Motion*, vol. 29, pp. 157–174, 1999.

[14] M. Ayub, M. H. Tiwana, and A. B. Mann, "Wiener-Hopf analysis of an acoustic plane wave in a trifurcated waveguide," *Archive of Applied Mechanics*, vol. 81, no. 6, pp. 701–713, 2010.

[15] B. Noble, *Methods Based on the Wiener-Hopf Technique*, Chelsea Publishing Company, New York, NY, USA, 2nd edition, 1988.

[16] J. B. Lawrie and I. D. Abrahams, "A brief historical perspective of the Wiener-Hopf technique," *Journal of Engineering Mathematics*, vol. 59, no. 4, pp. 351–358, 2007.

[17] R. V. Churchill and J. W. Brown, *Complex Variables and Applications*, McGraw-Hill, New York, NY, USA, 1996.

[18] D. S. Jones, *The Theory of Electromagnetism*, Pergamon Press, London, UK, 1964.

[19] A. Demír and A. Büyükaksoy, "Wiener-Hopf approach for predicting the transmission loss of a circular silencer with a locally reacting lining," *International Journal of Engineering Science*, vol. 43, no. 5-6, pp. 398–416, 2005.

[20] E. C. Titchmarsh, *Theory of Fourier Integrals*, Oxford University Press, Oxford, UK, 1937.

[21] R. Mittra and S. W. Lee, *Analytical Techniques in the Theory of Guided Waves*, Macmillan, New York, NY, USA, 1971.